ADVANCED FUNCTIONAL MATERIALS
www.afm-journal.de

Lipid-Containing Polymer Vesicles with pH/Ca^{2+}-Ion-Manipulated, Size-Selective Permeability

*Wen-Chia Huang, Wen-Hsuan Chiang, Su-Jen Lin, Yu-Jen Lan, Hsin-Lung Chen, Chorng-Shyan Chern, and Hsin-Cheng Chiu**

Polymeric vesicles attained from the self-assembly of distearin (a diacylglycerol lipid)-conjugated poly(acrylic acid) (PAAc) with various distearin contents in the aqueous phase show the capability of control over the vesicular-wall permeability to hydrophilic solutes of varying sizes by a simple manipulation of the external pH. The pH sensitivity of the vesicle membranes in size-selective permeability is largely dependent upon the lipid content of copolymer. By the addition of $CaCl_2$ in aqueous vesicle suspensions, the pH-evolved assembly structure and the membrane permeability can be immobilized with promoted resistance to further pH alteration, along with an additional counterion screening effect that reduces the pH required for the onset of polar solutes of certain sizes to pass through the membranes. Small-angle X-ray scattering (SAXS) measurements of the vesicle structure in the aqueous phase indicate that the pH-regulated permeability to polar solutes is virtually governed by the extent of hydration and swelling of the vesicle membranes, and the lipid residues within each vesicle wall are packed into the ≈4–5 repeating lamellar islet structure surrounded by PAAc segments.

1. Introduction

Self-assembly of amphiphilic copolymers into a vesicle structure (polymersomes) has attracted a great deal of interest due to their unique, well-controlled morphology in mimicking biological membranes, and potential applications as vehicles for needs where biphasic separation is required. These include the development of assemblies as carriers and bioreactors for drug delivery, catalysis, interface mediators, etc.[1–9] It is in great demand to develop polymer vesicles equipped with functional molecular apparatuses and/or the capability of undergoing pertinent morphological transitions in response to external stimuli.[10,11] For instance, polymer vesicles attained from the assembly of polybutadiene-*block*-poly(ethylene glycol) (PEG) diblock copolymers functionalized with nitrilotriacetic acid and tris(nitrilotriacetic acid) are capable of strongly associating with nickel(II), thereby providing specific recognition sites for the affinity adsorption of oligohistidine-tagged proteins on vesicular membranes.[12]

The transmembrane permeability is another important issue in the design of functional polymer vesicles. This can be achieved simply by the incorporation of pore-forming proteins within vesicular membranes.[13–15] The permeation of hydrophilic solutes can be either size selective or substrate specific, depending mainly on the transport mechanism of the inserted proteins. It is readily realized that the modulation of the membrane permeability achieved via the variation of the medium conditions (such as pH, temperature or chemicals) or external stimuli (temperature or magnetic field) can be advantageous, since this approach provides feasibility in controlling the functionality and promoting performance in a real-time, tunable manner.[5,11,16–18] Effective liberation of encapsulants from polymeric hollow spheres via structural responses in wall permeability enhancement or assembly dissociation to environmentally sensitive chemical reactions (oxidation, redox or hydrolysis) has been reported.[19–23] Many studies have demonstrated that a pH-induced change in the extent of the protonation of the ionizable groups within the copolymers that constitute the polymer vesicles allows a structural transformation in the vesicle walls, thereby leading to a dramatic change in the membrane permeability to hydrophilic cargoes.[24–30] Representing an important paradigm of this kind, polymer vesicles obtained from the self-assembly of the triblock copolymer PEG-*block*-polystyrene-*block*-poly(2-diethylaminoethyl methacrylate) (PDEA) have been shown to be capable of breathing (i.e., undergoing dramatic vesicle volume change) in response to pH. This was ascribed mainly to the pH-evolved water permeability

W.-C. Huang, S.-J. Lin, Y.-J. Lan
Department of Chemical Engineering
National Chung Hsing University
Taichung 402, Taiwan
Dr. W.-H. Chiang, Prof. H.-C. Chiu
Department of Biomedical Engineering and Environmental Sciences, National Tsing Hua University
Hsinchu 300, Taiwan
E-mail: hscchiu@mx.nthu.edu.tw
Prof. H.-L. Chen
Department of Chemical Engineering
National Tsing Hua University
Hsinchu 300, Taiwan
Prof. C.-S. Chern
Department of Chemical Engineering
National Taiwan University of Science and Technology
Taipei 106, Taiwan

DOI: 10.1002/adfm.201103117

increment across the membrane, which is intimately associated with the protonation at high pH of the PDEA blocks that were originally embedded as part of the hydrophobic regions within the vesicle walls.[28] In our previous work, polymer vesicles attained from the self-assembly of a copolymer composed of poly(acrylic acid) (PAAc) functionalized with 1,2-distearoyl-rac-glycerol (distearin) in an aqueous solution at pH = 5.0 were found to be capable of undergoing structural transformations that enhance the vesicular membrane permeability to calcein, a low-molecular-weight hydrophilic solute, in response to a dramatic pH change from 5.0 to 8.0.[30]

Herein, we show the first example of polymer vesicles with tailored membrane permeability to polar cargoes in a wide molecular weight range ≈600–70 000 g mol^{-1} in response to an external pH change. The polymer vesicles were developed from the spontaneous association of surface-active AAc-based copolymers prepared by the esterification of PAAc to varying degrees with distearin species (giving rise to a type of copolymer of AAc and distearin acrylate (DSA)). The pronounced effect of the DSA content of these copolymers on the susceptibility of the polymer vesicles in the size-selective permeability to pH is demonstrated. Through subsequent addition of $CaCl_2$ in aqueous vesicle suspensions, the pH-evolved vesicle structure could be immobilized, thereby leading to a stable vesicle structure with size-selective permeability to polar solutes with respect to further pH variation. This was notably accompanied with an additional counterion screening effect that reduced the pH required for the onset of polar solutes of certain sizes across the vesicle membranes. The pH-regulated permeability to polar solutes was governed by virtue of the hydration and swelling of the vesicle membranes, within which the lipid residues were arranged into a lamellar islet morphology surrounded by PAAc chain segments piling in a primary stack of ≈4–5 layers. This was confirmed by small-angle X-ray scattering (SAXS) measurements of the vesicle structure in the aqueous phase. The results obtained from this study are expected to provide a fundamental insight into the microstructural aspects of these novel polymer vesicles.

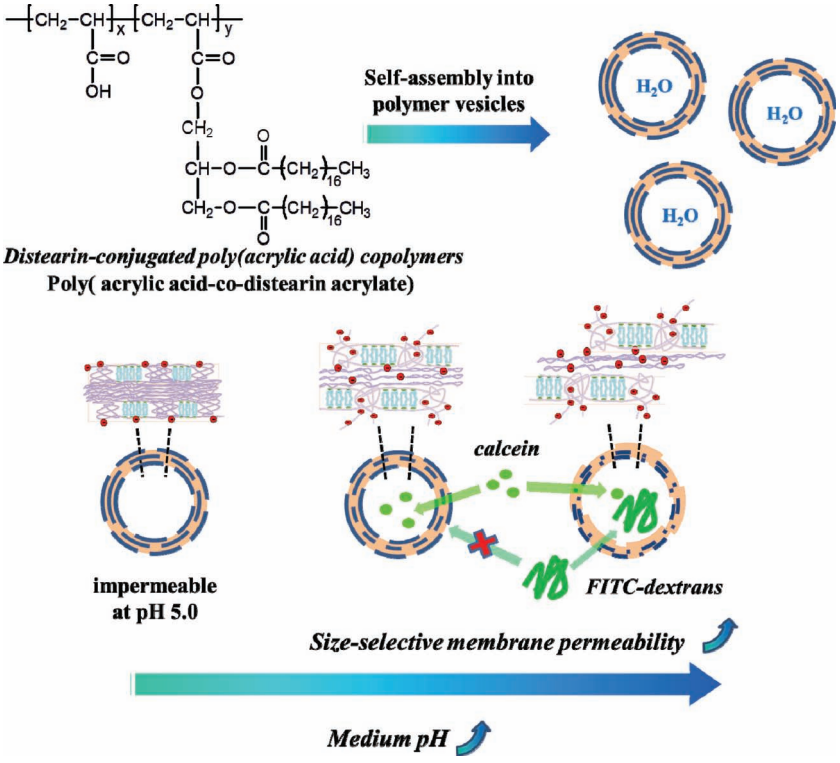

Scheme 1. Schematic illustration of polymer-vesicle assemblies equipped with pH-evolved size-selective permeability from self-association of hydrophobically modified PAAc (poly(AAc-*co*-DSA)).

2. Results and Discussion

Four copolymers with PAAc as the backbone, in which the AAc residues were partially conjugated with distearin to different extents via ester linkages, were employed for the vesicle preparation in this study. The copolymer structure is illustrated in **Scheme 1**. The synthesis recipes, compositions and average molecular weights of these copolymers are summarized in **Table 1**. Each copolymer is referred to by a copolymer identification code hereinafter. For example, PAAc-d8 refers to the

Table 1. Recipes, compositions and average molecular weights of the lipid-conjugated PAAc copolymers.

Copolymer	Reaction feed [mol%] NAS/distearin	DSA in copolymer [mol%]		M_w[a] [g mol^{-1}]
		^{1}H-NMR spectroscopy	Elemental analysis	
PAAc-d8	100/8	8.1 ± 0.6	7.8 ± 0.8	4.28×10^4
PAAc-d12	100/12	12.8 ± 1.1	12.3 ± 0.8	5.19×10^4
PAAc-d15	100/15	17.2 ± 1.9	15.4 ± 0.7	5.87×10^4
PAAc-d18	100/18	22.8 ± 2.2	18.3 ± 1.0	6.50×10^4

[a]Estimated by theoretical calculations as follows: backbone M_w = 25000 (g mol^{-1}) (M_w of PAAc by the GPC measurement after thorough hydrolysis of PNAS) + number of DSA × 679 (M_w of DSA).

copolymer comprising approximately 8 mol% of DSA and 92 mol% of AAc residues. The compositions were determined by both ^{1}H-NMR spectroscopy and elemental analysis in duplicate. The composition data for PAAc-d8 and PAAc-d12 were rather consistent between the two techniques. However, significant deviations in the copolymer composition occurred for PAAc-d15 and PAAc-d18, primarily as a result of self-association of the samples (most probably into the reversed micelle form) in $CDCl_3$ at ambient temperature during the ^{1} H-NMR spectroscopy characterization. This was confirmed by dynamic light scattering measurements (data not shown). The DSA contents in the copolymers were slightly higher than the corresponding molar ratios of the distearin to the *N*-acryloxysuccinimide (NAS) residues of polyNAS (PNAS) in the reaction feed. This was most likely caused by the thorough dialysis process for the purpose of purification. Being subjected to the double-emulsion ($w_1/o/w_2$) process, the copolymers could assemble supramolecularly into polymer vesicles in the microscale size range. **Figure 1**a–d shows laser-scanning confocal microscopy (LSCM) images of the four types of polymer vesicle in aqueous suspension. The vesicles in the images were revealed by the fluorescence of Nile red as a nonpolar probe associated with the vesicular membranes. The SEM images in Figure 1e and 1f also indicate the morphology of the lyophilized assemblies in hollow, spherical form. Being rather independent of which copolymer was used, the particle sizes were approximately 3.2 μm in radius, on average, estimated from at least 800 vesicles of the same batch by optical microscopy. Effective control of the vesicle size over a wide range from 1 to 15 μm could be attained simply by adjusting the tetrahydrofuran (THF)/$CHCl_3$ ratio, used as the organic phase during emulsification, as reported in our previous work.[30]

The formation of polymeric vesicles is largely governed by the balance of the hydrophilic/hydrophobic fractions of the amphiphilic copolymers employed.[31] In this study, the vesicle formation was driven by the hydrophobic packing of the distearyl tails of the DSA residues within the copolymer into the bilayer (or interdigitated) structure.[30] The un-ionized PAAc backbone segments could enhance the vesicle stability via extensive chain entanglement, hydrogen bonds and the spatial connections of the relatively closely packed lipid regions that they surrounded. Meanwhile, these slightly hydrated, un-ionized PAAc domains played a responsive role in triggering the morphological changes of the vesicular membranes upon alteration of the external pH. With the polymeric vesicles being produced in an aqueous solution of pH 5.0, those ionized AAc units resided mostly on the outer and inner surfaces of the vesicle membranes and thus prevented the vesicles from aggregating by the electrostatic repulsion mechanism (detailed structural analysis will be described below).

The permeability across the membranes of the vesicles prepared in aqueous solution at pH 5.0 (acetate buffer) to hydrophilic solutes was rather limited, irrespective of the copolymer and the hydrophilic fluorescence probe (including calcein (M_w = 622.6 g mol^{-1}) and fluorescein isothiocyanate-dextrans (FD) (series of 4, 10, 20, 40, 70 and 150 kDa)) employed in this study. **Figure 2**a illustrates the severe prohibition in the permeation of calcein (M_w = 622 g mol^{-1}) acting as a hydrophilic probe across the membranes of the vesicles produced from

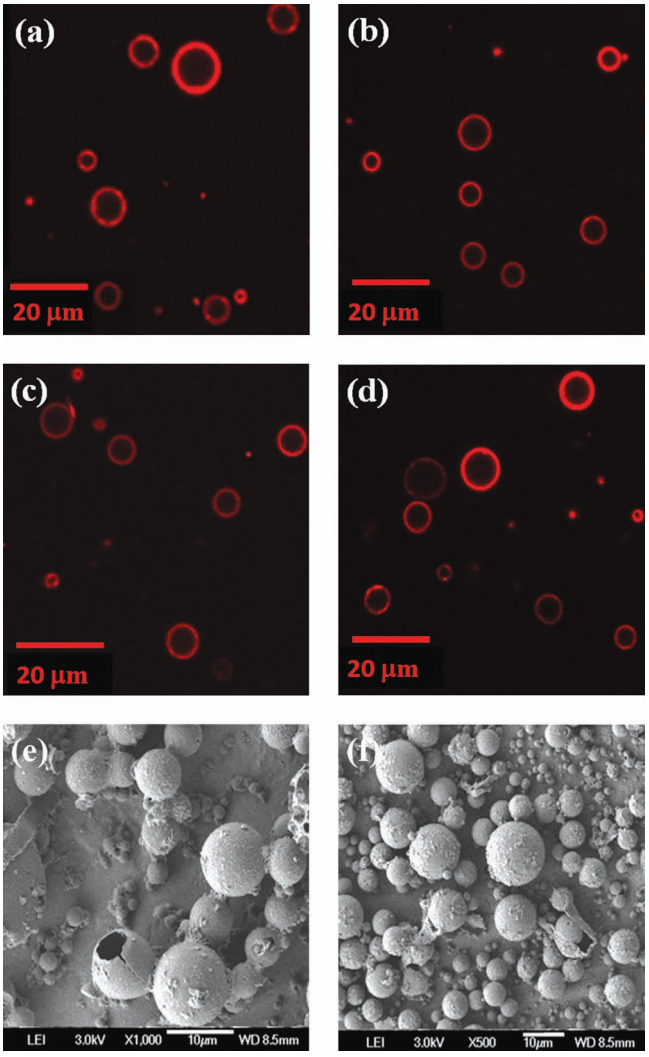

Figure 1. a–d) LSCM images of the Nile red-stained polymeric vesicles from self-assembly of the copolymers PAAc-d8 (a), PAAc-d12 (b), PAAc-d15 (c) and PAAc-d18 (d) in aqueous solutions with a pH of 5.0. e–f) SEM images of the lyophilized PAAc-d12 (e) and PAAc-d18 (f) hollow spheres.

PAAc-d8 at pH = 5.0. Similar results were also observed for the vesicles attained from the rest of the copolymers with higher DSA contents at pH = 5.0. This was obviously due to the relatively dense supramolecular packing of the copolymers into such a vesicular structure, with great integrity, which retarded the probe species from freely penetrating through the membranes. With the external pH being gradually increased to 6.8, the PAAc-d8 vesicles became permeable to calcein, as illustrated in Figure 2b. When the external aqueous solution of pH 6.8 was replaced with fresh acetate buffer of pH 5.0 (in the absence of calcein) within 2 h, the permeation process was again prohibited and the calcein was thus confined within the internal aqueous compartments of the vesicles (Figure 2c). A further increase in the pH of the medium of the PAAc-d8 vesicles to 7.4 enhanced the permeability and allowed FD4k and FD20k to pass through the vesicle membranes in addition to the calcein.

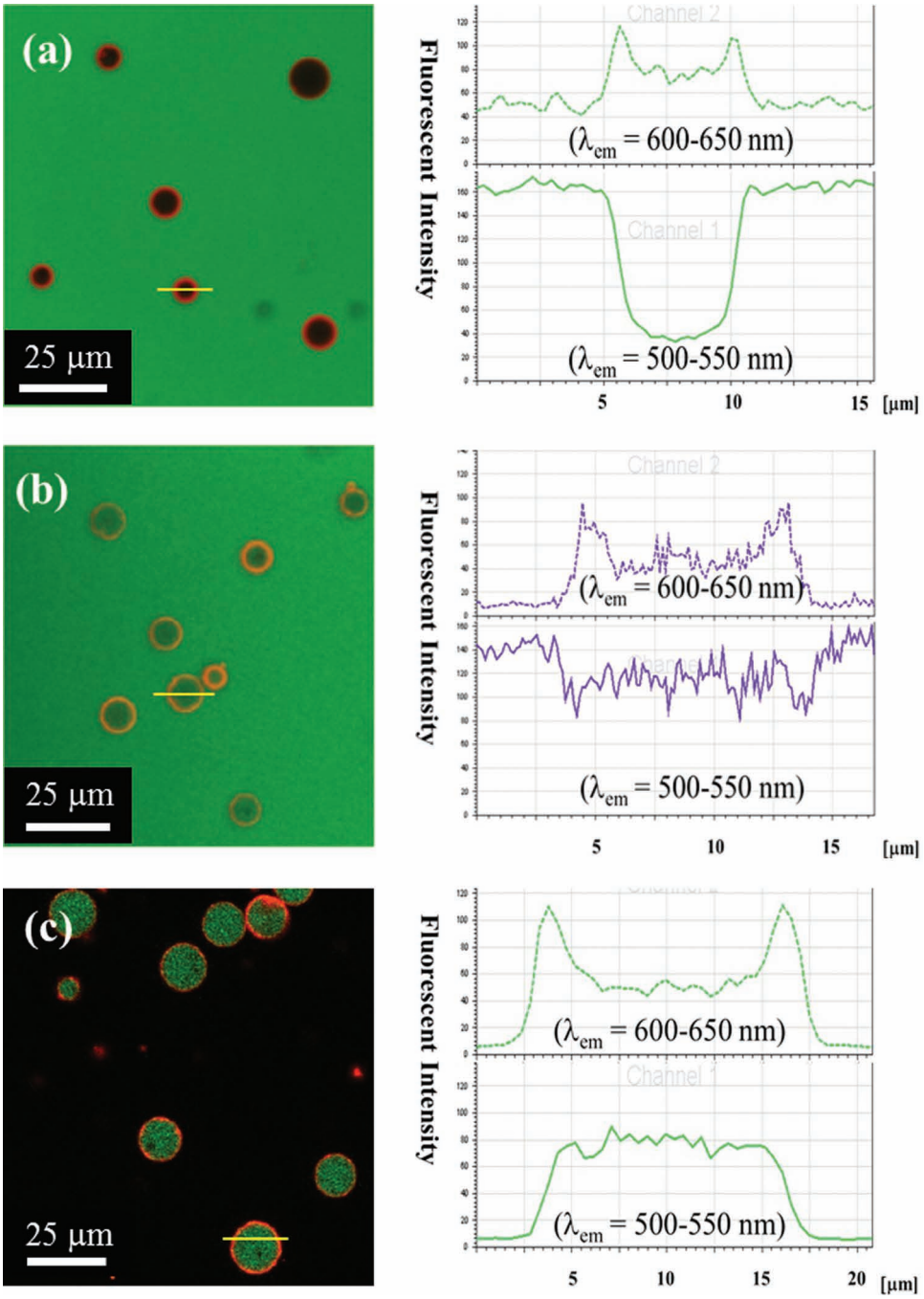

Figure 2. a–c) LSCM images and fluorescence intensity profiles of Nile red-stained PAAc-d8 vesicles in aqueous suspensions: on the addition of calcein at pH = 5.0 (diffusion into the vesicles is prohibited) (a); after pH adjustment to 6.8 (diffusion into the vesicles becomes feasible) (b); and after replacement of the external aqueous solution of pH 6.8 with fresh buffer of pH 5.0 (calcein is confined within the vesicles) (c).

However, vesicles assembled from PAAc-d12, PAAc-d15 and PAAc-d18 remained impermeable to calcein at pH = 6.8. The membrane permeability to calcein commenced at a higher pH of 8.0 for the PAAc-d12 vesicles. It was additionally enhanced when the pH was further increased from 8.0 to 8.8, at which point it became permeable to FD4k as well. In the still higher pH range of ≈8.8–9.5, the PAAc-d12 vesicle walls remained permeable to calcein and FD4k, but the passage of FD probes of higher molecular weights (FD20k and above) was severely restricted. In contrast, vesicles produced from PAAc-d15 and PAAc-d18 remained impermeable to calcein in the pH range of ≈5.0–9.5. Because hydrolysis of the ester linkage between the distearin and the PAAc backbone of the copolymers most likely takes place at high pH (i.e., above 9.5) by specific base catalysis, this degradation process inevitably leads to chemical disruption of the vesicle structure and, thus, severely restricts further

observations of vesicular permeability changes induced simply by the pH-evolved ionization of the AAc residues.

The above-mentioned results demonstrate that the vesicle-membrane permeability to hydrophilic cargoes of varying sizes was regulated simply by adjusting the pH of the medium. In addition, the susceptibility in this size-selective membrane permeability to pH was virtually governed by the DSA content of the copolymers used for the vesicle preparation. Furthermore, it was desirable to have a pH-evolved vesicle membrane structure that could be prominently immobilized, along with the preserved size-selective permeability, irrespective of further pH alteration. This could be achieved simply by the addition of $CaCl_2$ (5.0×10^{-3} M) into the aqueous vesicle suspensions immediately after the pH adjustment of the medium. The pH-evolved permeability of polymer vesicles could thus become invariable with either an increase or a decrease in the external pH. It should be noted that, by the addition of the $CaCl_2$, the onset pH that induced the free passage of calcein (which had the smallest size of the hydrophilic fluorescence probes utilized in this work) through the vesicle membranes decreased accordingly (e.g., from pH = 6.8 to pH = 6.3 for the PAAc-d8 vesicles). Similarly, the onset pH that allowed calcein to penetrate through the membranes of the PAAc-d12 vesicles was reduced from 8.0 to 7.8. Interestingly enough, the PAAc-d15 vesicles, with relatively dense membranes that were originally impermeable to all of the fluorescence probes in the pH range of ≈5.0 –9.5, became permeable to calcein at an onset pH of 8.5 when they were exposed to Ca^{2+} ions at a concentration of 5.0×10^{-3} M. In contrast, the PAAc-d18 vesicles remained inaccessible to calcein and all of the FD fluorescence probes chosen for the study in the pH range of ≈5.0–9.5, irrespective of the presence or absence of $CaCl_2$. The response of the permeability of the polymer vesicles in a polar solute to the pH change became more pronounced by the addition of $CaCl_2$, as compared with that in the absence of Ca^{2+} ions. For example, PAAc-d8 vesicles allowed FD4k, FD40k and even FD70k to diffuse through the membranes at corresponding onset pH values of 6.8, 7.2 and 7.4, respectively (**Table 2** and Figure S1, Supporting Information). A similar effect of Ca^{2+} cations on the PAAc-d12 vesicles for free membrane passage of FD4k in the pH range of ≈8.8–9.5 was observed. However, FD20k and those of larger sizes remained incapable of diffusing through the PAAc-d12 vesicle membranes. The membranes of the PAAc-d15 vesicles, which became accessible to calcein by the addition of $CaCl_2$ at pH = 8.5, still retained a structure that was impermeable to all of the FD fluorescence probes in the pH range of ≈8.5–9.5, in spite of the presence of Ca^{2+} ions. The pH dependence of the polar fluorescence probes permeating through the membranes of the polymer vesicles produced from the copolymers comprising various DSA contents is summarized in Table 2. The pronounced effect of the Ca^{2+} ions on the cooperatively enhanced permeability of the vesicle membranes accompanying the external pH manipulation was caused by the screening action of counterion pairings.[32] Appreciable condensation of the ionized PAAc backbone segments, originally acting as a blockade to solute penetration through the vesicle membranes, occurred, thus rendering the pH-evolved passage routes within the vesicle membranes as being more spacious for the facile transport of hydrophilic cargoes of larger sizes.

Table 2. The pH-evolved permeability of the polar fluorescence probes across the vesicle membranes in the presence of $CaCl_2$ (5.0×10^{-3}M), examined by LSCM. The numerical values represent the onset pH for the permeation of the fluorescence solute across the vesicular membranes. The PAAc-d18 vesicles were impermeable to all of the fluorescence solutes employed in the pH range of ≈5.0–9.5. Diffusion of FD150k across the vesicular membranes was prohibited by all of the polymer vesicles in the pH range of ≈5.0–9.5.

Vesicles	calcein	FD4K	FD20K	FD40K	FD70K
PAAc-d8	6.3	6.8	7.2	7.2	7.4
PAAc-d12	7.8	8.8	NA	NA	NA
PAAc-d15	8.5	NA[a)]	NA	NA	NA

[a)] Not applicable/impermeable.

As mentioned above, after the desired membrane permeability had been attained by pH adjustment, the subsequent addition of Ca^{2+} ions into the aqueous vesicle suspensions could prominently immobilize the vesicle structure and maintain the satisfactory membrane permeability as well. The vesicle membranes could thus become permeable only to calcein at either pH = 5.0 or 9.5. Taking the PAAc-d8 vesicles as an example, the goal could be achieved simply by the adjustment of the external pH to 6.3 and then the addition of $CaCl_2$. This was followed by a further change in the external pH from 6.3 to either 5.0 or 9.5. Similarly, except for FD150k, the polar fluorescence probes exploited herein became capable of freely diffusing across the membranes of the PAAc-d8 vesicles in the full pH range of ≈5.0 –9.5 upon the pH/Ca^{2+}-based manipulation of the membrane structure. The immobilization of the vesicle structure by Ca^{2+} ions was caused primarily by partial cross-linking of the polymer chain segments arising from the electrostatic attraction of divalent cations with the ionized carboxylate groups of the AAc residues. A similar effect of Ca^{2+} ions on the transformation of alginate in the aqueous phase from the dissolved state to the gel state is well documented.[33,34] In contrast, this "lock-up" action of Ca^{2+} ions on the vesicle structure and permeability could be readily released by further addition of, for example, ethylenediaminetetra-acetic acid (EDTA) into the aqueous vesicle suspensions at a concentration of 3.0×10^{-3} M. The capability of the resultant vesicles of undergoing the membrane structure transformation and the corresponding permeability regulation in response to external pH changes were then restored. This was caused primarily by the replacement of AAc carboxylates with EDTA for cationic chelation and, thus, the release of the lock-up action in the vesicle structure.

The membrane structure of the polymer vesicles as a function of pH, developed herein, was further investigated by SAXS. **Figure 3** shows the SAXS profiles of the vesicles having three different DSA contents, at pH = 5.0 in the presence of Ca^{2+} ions (5.0×10^{-3} M) in the aqueous phase. The scattering profile of the PAAc-d8 vesicles exhibits sharp characteristic Bragg peaks ($n\lambda = 2d\sin\theta$, n = 001, 002, 003...), thereby illustrating a repeated lamellar structure within the single-wall membrane of each vesicle, with the lamella number in the range of ≈4–5 and an interlamellar d-spacing ($2\pi/q$, where q denotes the scattering vector) of approximately 7.04 nm.[35,36] The lamella number was estimated by the Debye–Scherrer relation, $L_m = 2\pi/\Delta q$, where

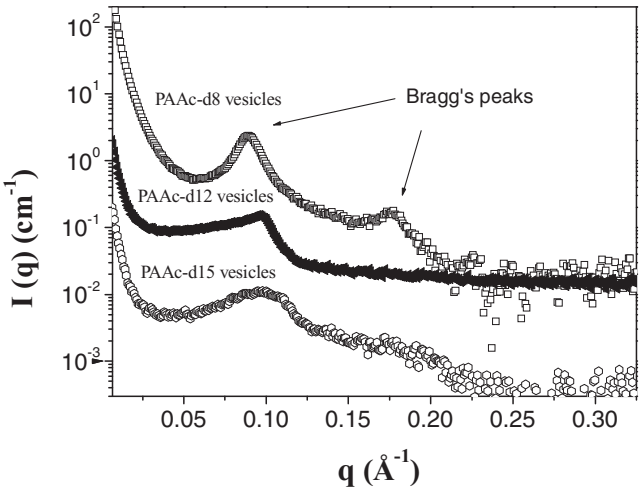

Figure 3. SAXS profiles of polymer vesicles with different DSA contents in aqueous solutions at pH = 5.0 in the presence of $CaCl_2$ (5.0×10^{-3} M).

Δq is the experimental full width at half-maximum (FWHM) of the (001) Bragg peak in q space.[37,38] The average domain size of the multilayers (vesicular membrane thickness), L_m, thus obtained was approximately 31.0 nm. This gave rise to vesicle membranes with an ≈4–5 (4.4 on average) repeating-lamella morphology. These data strongly suggest that the lamellar phases, in which each comprised alternating DSA bilayer islets and relatively more hydrated AAc-rich domains, were built up repeatedly into a multilayer structure with a periodicity $d = 2\pi/q_{001} \approx 7.04$ nm.

The SAXS profiles displayed broader scattering peaks at q = 0.079 and 0.078 Å^{-1} for the PAAc-d8 vesicles in aqueous phases with pH = 6.8 and 7.4, respectively, than that at q = 0.089 Å^{-1} and pH = 5.0; meanwhile, the Bragg pattern still remained notable (**Figure 4**). The feature spacing of the multilayer structure was enlarged from 7.04 to 8.00 (or to 8.08) nm corresponding to a change of pH from 5.0 to 6.8 (or to 7.4), while the assembly

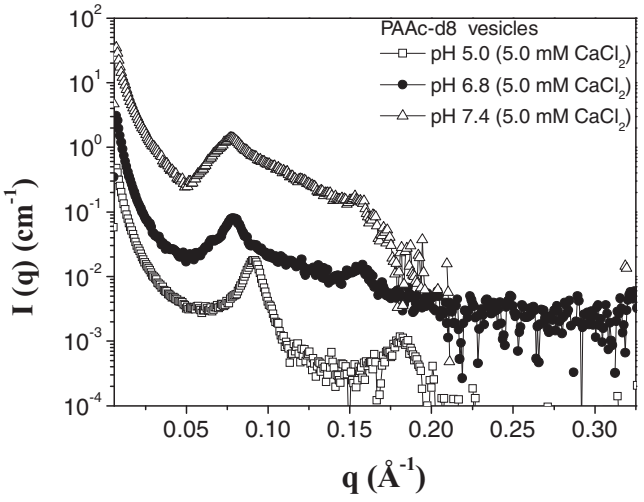

Figure 4. SAXS profiles of the PAAc-d8 vesicles in aqueous suspensions at pH = 5.0, 6.8 and 7.4 in the presence of $CaCl_2$ (5.0×10^{-3} M).

was maintained in a vesicular structure, as confirmed by LSCM (Figure S1, Supporting Information). In addition, the characteristic scattering peak of the PAAc-d8 vesicles in the SAXS profiles was somewhat broadened as the pH was increased from 5.0 to 7.4 (Figure 4), implying that the PAAc-d8 vesicle membrane underwent a morphological transition from originally 4 or 5 layers to a mixture with fewer repeating lamellae. It is postulated that, with the self-association of the copolymer into a vesicle morphology at pH = 5.0, the membranes are composed of a discrete multilayer architecture (with ≈4 –5 layers), built up of alternating DSA bilayers and interfacial AAc-rich domains that are intimately surrounded by transmembrane, un-ionized, AAc-rich regions within the interior of the membranes. The ionized AAc units are mostly accommodated on the most outer and inner membrane surfaces. When the pH of the medium is raised, the ionization degree of AAc residues is increased accordingly. As a consequence, the AAc-rich domains become more hydrated and swollen, inevitably leading to the expansion of the interlayer spacing of the multilamellar structure, or even a slight disruption of the multilayer structure, which occurs exclusively in the PAAc-d8 vesicles (due to the lowest DSA content among all of the copolymers investigated in this study). Acting as pH-responsive channels, the transmembrane, AAc-rich regions also become accessible to hydrophilic cargoes of certain sizes, which can penetrate through the membrane as the ionization extent is increased. Scheme 1 represents a schematic model for the pH-evolved morphological transformation and the formation of size-selective channels within the vesicle membranes.

In spite of the absence of the Bragg pattern that has been frequently observed for the multilamellar lipid bilayer structure in the aqueous phase,[39,40] the SAXS profiles of the PAAc-d12 and PAAc-d15 vesicles showed rather sharp scattering-intensity peaks at higher q positions, compared with those of the PAAc-d8 vesicles at pH = 5 (Figure 3). This suggests that both the PAAc-d12 and PAAc-d15 vesicles were in the multilayer form, with reduced interlayer d-spacings (6.29 and 6.19 nm, as characterized by scattering peaks at q = 0.100 and 0.102 Å^{-1}, respectively). The interlayer d-spacing of the PAAc-d8 vesicles was 7.04 nm, as determined from the scattering peak at q = 0.089 Å^{-1}. The decreased lamellar d-spacing resulted primarily from the reduced dimensions of the AAc-rich domains residing within the interfacial regions among the distearin lamellae, by virtue of a decrease in the AAc residues that were available for formation of these microdomains, along with the copolymers comprising increased DSA units. This is in agreement with the observation that the higher the DSA content of the copolymer was, the higher was the pH required to induce sufficient ionization of the AAc residues and disrupt the close packing of the PAAc backbone segments with the lipid bilayer structure within the vesicle membranes. On the other hand, based on the Debye–Scherrer postulation, the PAAc-d12 vesicle membrane with $L_m \approx 25.1$ nm, calculated from the FWHM of the first-order lamellar peak in Figure 3, was composed of approximately four repeating polymer layers, comparable with that of the PAAc-d8 vesicles at pH = 5.0. For the PAAc-d15 vesicles, the primary scattering peak of the SAXS profiles was slightly broader than that of PAAc-d8 vesicles at pH = 5.0. Because of the increased hydrophobicity of the vesicle-membrane structure

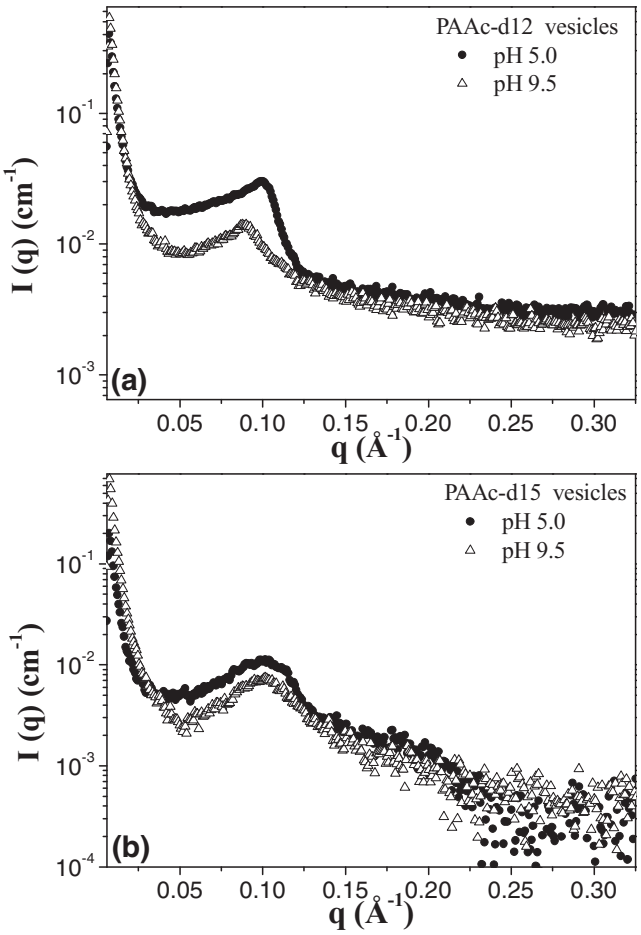

Figure 5. a,b) SAXS profiles of PAAc-d12 (a) and PAAc-d15 (b) in aqueous suspensions at pH = 5.0 and 9.5, respectively, in the presence of $CaCl_2$ (5.0×10^{-3} M).

with increasing DSA content of copolymer, the interior of the vesicle membranes became more immensely dehydrated and solidified at a faster structural development rate. This would then lead to the collapse of the lamellae in the absence of the full transition from a disordered to an ordered arrangement of the multilayer structure. This was accompanied by a slight increase in the breadth of the multilayer distribution and the limitation of precisely evaluating the FWHM from the SAXS profile, and thus the lamellar number.

Note that PAAc-d12 and PAAc-d15 vesicles retained the multilayer architecture (essentially unchanged) within each wall membrane in the pH range of ≈5.0 –9.5, as evidenced by their relatively sharp scattering peaks in the SAXS profiles, in spite of the absence of the Bragg pattern (**Figure 5**). This reflects the enhanced membrane integrity of the vesicles produced from the copolymers with higher DSA contents against the external pH fluctuation. However, Figure 5a shows that the PAAc-d12 vesicle membranes became slightly swollen (which most likely occurred in the AAc-rich domains) in response to a pH change from 5.0 to 9.5, thereby leading to the increased *d*-spacing feature of the multilayer structure from 6.29 to 7.06 nm. Such a pH-evolved change in the membrane morphology allowed the permeation of FD4k across the vesicular membranes. On the other hand, the difference in the *q* positions associated with the characteristic scattering peaks in the SAXS profiles of the PAAc-d15 vesicles at pH = 5.0 and 9.5 was rather insignificant (Figure 5b). This implies only a negligible variation in the prominently stabilized multilayer arrangement, with the *d*-spacing remaining approximately unchanged at approximately 6.19 nm, even though pH-induced hydration of the AAc-rich regions (particularly within the transmembrane zone) occurred to some extent. As expected from the interlayer *d*-spacing characterization, the layered structure of the PAAc-d15 vesicle membranes still remained closely packed, and the slightly swollen AAc-rich regions solely allowed small fluorescence probes such as calcein to pass through in response to a pH change from 5.0 to 9.5.

3. Conclusions

Polymeric vesicles attained from the spontaneous association of copolymers comprising AAc and different levels of DSA residues in the aqueous phase showed controllable membrane permeability to hydrophilic solutes of various sizes by simple manipulation of the external pH. The pH-evolved size-selective permeability of the vesicular membranes was virtually governed by the DSA content of copolymer and the addition of Ca^{2+} cations. By the addition of $CaCl_2$ into the aqueous vesicle suspensions immediately after the pH adjustment of the medium, the pH-evolved assembly structure was immobilized accordingly. Under these circumstances, the permeability became pH-independent, along with an additional counterion screening effect that somewhat enlarged the passage routes in the spaces within membranes for polar solutes to pass through. SAXS measurements of the vesicle structures in the aqueous phase indicate that the pH/Ca^{2+} -ion-induced permeability was governed by the extent of hydration and swelling of the vesicle membranes in an ≈4–5 repeating lamellar morphology.

4. Experimental Section

Synthesis and Characterization of Lipid-Containing Copolymers: PNAS was prepared by radical polymerization of NAS in *N*,*N*-dimethylformamide (DMF), using 2,2'-azoisobutyronitrile (AIBN) as an initiator, at 60 °C for 20 h, with stirring under a nitrogen atmosphere. The PNAS was purified by precipitation twice from acetone, collected by filtration and then dried in vacuo.[41,42] Poly(AAc-*co*-DSA) was obtained firstly by partial transesterification of the PNAS with distearin in a dimethyl sulfoxide (DMSO)/pyridine (1/2, v/v) solution at 60 °C for 72 h in the presence of 4-dimethylaminopyridine as a catalyst. This was followed by thorough hydrolysis of the unreacted NAS residues of the copolymer into the AAc units at 40 °C for 5 d by addition of 2-amino-2-hydroxymethyl-propane-1,3-diol (tris) buffer (pH = 8.5; an equal amount to the original reaction solution volume) into the polymer solution. The crude product was then subjected to dialysis (Spectra/Por molecular weight cut-off (MWCO) ≈ 6000–8000) at 4 °C under stirring against DMSO/THF solution (2/1, v/v) for 5 d and then deionized water for 7 d, in sequence. The final product was collected by lyophilization. The polymer structure was characterized using ^{1}H-NMR spectroscopy (Varian Unity Inova-600, 600 MHz) in $CDCl_3$ at ambient temperature, using DMF in a sealed capillary coaxially placed within the sample tube as the external standard (representatively illustrated in Figure S2, Supporting Information). The calibration established for calculating the

polymer composition was obtained from the relative signal integrals of the distearin in $CDCl_3$ (six concentrations) at $\delta = 0.865$ ppm, with respect to the integral of DMF at $\delta = 8.49$ ppm. The compositions were also determined by elemental analysis on the oxygen and carbon atoms of the copolymers, after thorough sample drying under vacuum. The purity was confirmed by gel-permeation chromatography (GPC) (Agilent 1100, PL-gels columns in series: GP-503; separation range 500–60k and GP-504; ≈10k–600k) using THF as the eluent at a flow rate of 1.0 mL min^{-1} under refractive-index (RI) detection (Agilent 1100). The weight-average molecular weight (2.5×10^4 g mol^{-1}) and polydispersity (1.68) of the resulting poly(AAc), after thorough hydrolysis of the PNAS, which was employed as a reactive polymeric precursor for covalent attachment of distearin throughout this study, were determined by GPC (PL-Aquagel-OH columns in series: GF083; 100–30k, GF084; 10k–200k, and GF086; 200k–10M, calibrated with poly(sodium acrylate) standards) using boric buffer (0.1 M NaCl, pH = 9.0) as the eluent at a flow rate of 1.0 mL min^{-1} under RI detection. The average molecular weights of the copolymers were obtained from the molecular weight of PAAc and the molar contents of DSA within the copolymers.

Polymer-Vesicle Preparation: The polymer vesicles were prepared according to a method described elsewhere, with slight modification.[30] The copolymer (5.0 mg) was firstly dissolved in an organic cosolvent system (5.0 mL) comprising THF and chloroform (20/80, v/v). The solution was then vigorously mixed with an acetate buffer solution (ionic strength 0.01 M, pH = 5.0, 2.5 mL) using a homogenizer (Ika, T18) at 6000 rpm in an ice/water bath for 4 min to produce an intermediate w/o emulsion. The emulsion was immediately added into excess acetate buffer (identical to the w_1 phase) at 20 °C with magnetic stirring to develop a $w_1/o/w_2$ emulsion. The stirring continued until complete removal of the organic solvents (no detectable cosolvents after approximately 6 h). The resultant aqueous vesicle suspension was concentrated by ultrafiltration to give a final volume of approximately 5 mL.

Polymer-Vesicle Characterization: The permeability of the polymer-vesicle membranes to hydrophilic solutes of varying sizes as a function of the external pH was conducted on a Carl Zeiss LSM510 LSCM with a Plan-Apochromat 63-oil immersion objective (numerical aperture (NA) = 1.4) and Pascal software. The vesicle suspensions were stained with Nile red (λ_{ex} = 543 nm, λ_{em} = 600–700 nm) (2.0×10^{-7} M) as the hydrophobic membrane-associated probe. The pH of the medium was adjusted from 5.0 (at which the vesicles were produced) to the desired value using 0.1 N KOH. For the experiment regarding vesicle structure immobilization by Ca^{2+} ions, $CaCl_2$ was added to the vesicle suspension to a final concentration of 5.0×10^{-3} M immediately after the pH adjustment to the prescribed value. This was followed by the addition of a water-soluble fluorescence probe serving as a polar cargo into the polymer vesicle suspension. Images of water-soluble probes in the vesicle suspensions obtained from LSCM with an excitation at 488 nm and emission range of ≈505–550 nm were superimposed with those attained from Nile red for the permeability evaluation. The number-average size of the polymer vesicles on the micrometer scale was evaluated on the basis of at least 800 vesicles, from images from an inverted optical microscope (Olympus, IX70) equipped with a digital camera (Canon), using Image-Pro Plus software (version 4.5, Media, Cybernetic). Examination of the dried, hollow polymer microspheres was conducted using a JEOL JSM-6700F field-emission scanning electron microscope (FE-SEM) after the lyophilized samples were coated with Au. For the SAXS analysis, samples were run at beamline 23A1 at the National Synchrotron Radiation Research Center (NSRRC), Hsinchu, Taiwan. For the SAXS experiments, the energy of X-ray source was 14 keV. The scattering signals were collected using a MarCCD detector with a pixel resolution of 512 × 512. The scattering intensity profiles were depicted from the scattering intensity (I) versus scattering vector, $q = (4\pi/\lambda)\sin(\theta/2)$ (where θ is the scattering angle), after corrections for solvent background, sample transmission, empty cell transmission, empty cell scattering and the detector sensitivity.[43] For the static experiments, small amounts of the polymeric vesicular suspension (5.0 mg mL^{-1}) at a preset pH were placed in the center of a steel washer, closely sealed with Kapton tape and run for 5 min. All of the data were normalized and the background corrected before analysis.

Supporting Information

Supporting Information is available from the Wiley Online Library or from the author.

Acknowledgements

This work was financially supported by the National Science Council (NSC99-2627-M-007-009 and NSC99-2221-E-007-006-MY3) and the National Tsing Hua University (100N2053E1) of Taiwan. The authors also thank the National Synchrotron Radiation Research Center (Hsinchu, Taiwan) for the use of LSCM and SAXS (23A1).

Received: December 22, 2011
Published online: March 13, 2012

[1] H. Iatrou, H. Frielinghaus, S. Hanski, N. Ferderigos, J. Ruokolainen, O. Ikkala, D. Richter, J. Mays, N. Hadjichristidis, *Biomacromolecules* **2007**, *8*, 2173.
[2] W. Y. Ayen, K. Garkhal, N. Kumar, *Mol. Pharmaceutics* **2011**, *8*, 466.
[3] A. Kishimura, A. Koide, K. Osada, Y. Yamasaki, K. Kataoka, *Angew. Chem.* **2007**, *119*, 6197; *Angew. Chem. Int. Ed.* **2007**, *46*, 6085.
[4] G. J. Liu, S. B. Ma, S. K. Li, R. Cheng, F. H. Meng, H. Y. Liu, Z. Y. Zhong, *Biomaterials* **2010**, *31*, 7575.
[5] K. T. Kim, J. J. L. M. Cornelissen, R. J. M. Nolte, J. C. M. van Hest, *Adv. Mater.* **2009**, *21*, 2787.
[6] H. Lomas, A. P. Johnston, G. K. Such, Z. Zhu, K. Liang, M. P. van Koeverden, S. Alongkornchotikul, F. Caruso, *Small* **2011**, *7*, 2109.
[7] A. L. Becker, A. P. Johnston, F. Caruso, *Small* **2010**, *6*, 1836.
[8] B. Stadler, A. D. Price, A. N. Zelikin, *Adv. Funct. Mater.* **2011**, *21*, 14.
[9] K. H. Liu, S. Y. Chen, D. M. Liu, T. Y. Liu, *Macromolecules* **2008**, *41*, 6511.
[10] N. P. Kamat, G. P. Robbins, J. Rawson, M. J. Therien, I. J. Dmochowski, D. A. Hammer, *Adv. Funct. Mater.* **2010**, *20*, 2588.
[11] A. Blanazs, M. Massignani, G. Battaglia, S. P. Armes, A. J. Ryan, *Adv. Funct. Mater.* **2009**, *19*, 2906.
[12] R. Nehring, C. G. Palivan, S. Moreno-Flores, A. Mantion, P. Tanner, J. L. Toca-Herrera, A. Thunemann, W. Meier, *Soft Matter* **2010**, *6*, 2815.
[13] M. Sauer, T. Haefele, A. Graff, C. Nardin, W. Meier, *Chem. Commun.* **2001**, 2452.
[14] P. Broz, S. Driamov, J. Ziegler, N. Ben-Haim, S. Marsch, W. Meier, P. Hunziker, *Nano Lett.* **2006**, *6*, 2349.
[15] M. Nallani, S. Benito, O. Onaca, A. Graff, M. Lindemann, M. Winterhalter, W. Meier, U. Schwaneberg, *J. Biotechnol.* **2006**, *123*, 50.
[16] S. Ihle, O. Onaca, P. Rigler, B. Hauer, F. Rodriguez-Ropero, M. Fioroni, U. Schwaneberg, *Soft Matter* **2011**, *7*, 532.
[17] H. F. Xu, F. H. Meng, Z. Y. Zhong, *J. Mater. Chem.* **2009**, *19*, 4183.
[18] C. Sanson, O. Diou, J. Thevenot, E. Ibarboure, A. Soum, A. Brulet, S. Miraux, E. Thiaudiere, S. Tan, A. Brisson, V. Dupuis, O. Sandre, S. Lecommandoux, *ACS Nano* **2011**, *5*, 1122.
[19] S. Cerritelli, D. Velluto, J. A. Hubbell, *Biomacromolecules* **2007**, *8*, 1966.
[20] A. Napoli, M. Valentini, N. Tirelli, M. Muller, J. A. Hubbell, *Nat. Mater.* **2004**, *3*, 183.
[21] Y. J. Ma, W. F. Dong, M. A. Hempenius, H. Mohwald, G. J. Vancso, *Nat. Mater.* **2006**, *5*, 724.
[22] Y. Q. Shen, E. L. Jin, B. Zhang, C. J. Murphy, M. H. Sui, J. Zhao, J. Q. Wang, J. B. Tang, M. H. Fan, E. Van Kirk, W. J. Murdoch, *J. Am. Chem. Soc.* **2010**, *132*, 4259.
[23] Z. Cheng, A. Tsourkas, *Langmuir* **2008**, *24*, 8169.
[24] J. Du, S. P. Armes, *J. Am. Chem. Soc.* **2005**, *127*, 12800.

[25] Y. F. Zhu, J. L. Shi, W. H. Shen, X. P. Dong, J. W. Feng, M. L. Ruan, Y. S. Li, *Angew. Chem.* **2005**, *117*, 5213; *Angew. Chem. Int. Ed.* **2005**, *44*, 5083.
[26] W. J. Tong, C. Y. Gao, H. Mohwald, *Macromolecules* **2006**, *39*, 335.
[27] E. G. Bellomo, M. D. Wyrsta, L. Pakstis, D. J. Pochan, T. J. Deming, *Nat. Mater.* **2004**, *3*, 244.
[28] S. Y. Yu, T. Azzam, I. Rouiller, A. Eisenberg, *J. Am. Chem. Soc.* **2009**, *131*, 10557.
[29] M. S. Kim, D. S. Lee, *Chem. Commun.* **2010**, *46*, 4481.
[30] H. C. Chiu, Y. W. Lin, Y. F. Huang, C. K. Chuang, C. S. Chern, *Angew. Chem.* **2008**, *120*, 1901; *Angew. Chem. Int. Ed.* **2008**, *47*, 1875.
[31] F. Ahmed, P. J. Photos, D. E. Discher, *Drug Dev. Res.* **2006**, *67*, 4.
[32] H. C. Chiu, Y. F. Lin, S. H. Hung, *Macromolecules* **2002**, *35*, 5235.
[33] A. Kikuchi, M. Kawabuchi, M. Sugihara, Y. Sakurai, T. Okano, *J. Controlled Release* **1997**, *47*, 21.
[34] H. G. Zhu, R. Srivastava, M. J. McShane, *Biomacromolecules* **2005**, *6*, 2221.
[35] C. M. Wu, H. L. Chen, W. Liou, T. L. Lin, U. S. Jeng, *Biomacromolecules* **2004**, *5*, 2324.
[36] U. S. Jeng, C. H. Hsu, T. L. Lin, C. M. Wu, H. L. Chen, L. A. Tai, K. C. Hwang, *Physica B* **2005**, *357*, 193.
[37] D. Pozzi, G. Caracciolo, R. Caminiti, S. C. De Sanctis, H. Amenitsch, C. Marchini, M. Montani, A. Amici, *ACS Appl. Mater. Interfaces* **2009**, *1*, 2237.
[38] H. Amenitsch, G. Caracciolo, P. Foglia, V. Fuscoletti, P. Giansanti, C. Marianecci, D. Pozzi, A. Lagana, *Colloids Surf. B: Biointerfaces* **2011**, *82*, 141.
[39] G. Pabst, *Biophys. Rev. Lett.* **2006**, *1*, 57.
[40] G. Pabst, R. Koschuch, B. Pozo-Navas, M. Rappolt, K. Lohner, P. Laggner, *J. Appl. Crystallogr.* **2003**, *36*, 1378.
[41] Y. H. Hsu, W. H. Chiang, C. H. Chen, C. S. Chern, H. C. Chiu, *Macromolecules* **2005**, *38*, 9757.
[42] W. H. Chiang, Y. H. Hsu, C. S. Chern, H. C. Chiu, *Polymer* **2011**, *52*, 2422.
[43] C. Y. Chen, S. H. Chan, J. Y. Li, K. H. Wu, J. H. Chen, W. Y. Huang, S. A. Chen, H. L. Chen, *Macromolecules* **2010**, *43*, 7305.